Astrophys Space Sci (2007) 311: 111–115
DOI 10.1007/s10509-007-9533-5

ORIGINAL ARTICLE

Galactic winds from primeval galaxies

Masao Mori · Masayuki Umemura

Received: 30 March 2007 / Accepted: 27 May 2007 / Published online: 8 June 2007

Abstract Ultra-high resolution hydrodynamic simulations using 1024^3 grid points are performed of early supernova burst in a forming galaxy, with properties similar to those inferred for Lyman α emitters (LAEs) and Lyman Break Galaxies (LBGs). We show that, at the earliest stages of less than 300 Myr, continual supernova explosions produce multitudinous hot bubbles and cooled H(I) shells in-between. The H(I) shells radiate intense Lyman α (Lyα) emission like LAEs. We found that the bubbly structures produced are quite similar to the observed features in the Lyα surface brightness distribution of the extended LAEs. After 1 Gyr, the galaxies are dominated by stellar continuum radiation and then resemble the LBGs. At this point, the abundance of heavy elements appears to be solar. After 13 Gyr, these galaxies resemble present-day ellipticals.

Keywords Galaxy formation · Chemical evolution · Hydrodynamics

1 Introduction

Recent observations have revealed the presence of a number of LAEs at redshifts of $z \geq 3$ (Dey et al. 1998; Tanighichi et al. 2003 and references therein) as well as LBGs at redshifts of $3 \leq z \leq 6$ (Steidel et al. 1996; Giavalisco 2002 and references therein). Since LAEs and LBGs are quite young, they could hold direct interpretable information on the early chemical enrichment of galaxies, contrary to present-day galaxies which have undergone intense interstellar medium (ISM) recycling, thus erasing most of the early chemical history. Therefore, high redshift LAEs and LBGs possibly provide a significant key for the chemical and dynamical evolution of galaxies. LBGs have been argued as candidate progenitors of present-day elliptical galaxies in terms of their observed properties. But, what evolutionary stages LBGs correspond to and how they are related to LAEs are still under debate.

The modern paradigm of the galaxy formation, based on the cold dark matter hypothesis, deduces that galaxies formed hierarchically in a bottom-up fashion, where a larger system results from the assembly of smaller dark matter halos (Blumenthal et al. 1984). Recent developments in computer technologies and numerical methods have made it possible to simulate the multi-dimensional dynamical or chemodynamical evolution of galaxies including the collisionless dynamics of the dark matter and the effect of star formation and supernova (SN) feedback. A dynamical, chemical, and spectrophotometric scheme has become a powerful tool to explore the formation and evolution of galaxies (Mori et al. 1997, 1999).

In this paper, we report a high-resolution simulation that follows dynamical and chemical evolution from the earliest stages of galaxy formation through the period of dynamical relaxation (e.g. Mori and Umemura 2006). The outline of this paper is as follows. In Sect. 2, we present the simulation model and the results are described in Sect. 3. The possible link among LAEs, LBGs and elliptical galaxies is discussed in Sect. 4.

M. Mori (✉)
Institute of Natural Sciences, Senshu University,
Kawasaki 214-8580, Japan
e-mail: mmori@isc.senshu-u.ac.jp

M. Umemura
Center for Computational Sciences, University of Tsukuba,
Tsukuba 305-8577, Japan

2 Model

Following a standard cold dark matter cosmology with cosmological constant (ΛCDM), where we assume $\Omega_M = 0.3$, $\Omega_\Lambda = 0.7$, $\Omega_b = 0.04$, and a Hubble constant of $H_0 = 70\,\mathrm{km\,s^{-1}\,Mpc^{-1}}$, we consider the dynamical and chemical evolution of a protogalaxy with the total mass of $10^{11} M_\odot$. We assumed that the total mass of gaseous matter is $1.3 \times 10^{10} M_\odot$ initially. Here, we consider the evolution of a relatively isolated 2σ density fluctuation in the ΛCDM universe with sub-galactic dark halos originating from 2σ density fluctuations. In this case, sub-galactic dark matter halos with the mass of $\sim 5 \times 10^9 M_\odot$ collapse and virializes at the redshift $z = 7.8$. On the other hand, a dark matter halo with the mass of $10^{11} M_\odot$ decouples from the cosmic expansion and begins to collapse at the same redshift. In the light of these points, we simply model a protogalaxy with the total mass of $10^{11} M_\odot$ as an assemblage of sub-galactic condensations with a mass of $5 \times 10^9 M_\odot$ in a virial radius 8.6 kpc. The galaxy as a whole is modeled as a pre-virialized system in a radius of 53.7 kpc. Subgalactic condensations having a zero velocity are then distributed randomly (see Fig. 1). These are taken as already virialized systems with a Navarro-Frenk-White density profile (Navarro et al. 1997). The angular momentum is provided by a uniform rotation characterized by a spin parameter of $\lambda = 0.05$ (Barnes and Efstathiou 1987).

Our simulations use a hybrid collisionless N-body plus gas hydrodynamic code which is applicable to a complex system consisting of dark matter, stars and gas. The gas is allowed to form stars and is subject to physical processes such as the radiative cooling and the energy feedback from supernovae and massive stars. Chemical and photometric evolution of the system can also be simulated by this code. The collisionless dynamics for dark matter particles is treated by the N-body method. The gas dynamics is pursued by a three-dimensional hydrodynamic scheme with 1024^3 Cartesian grids. The simulation box has a (physical) size of 134 kpc and the spatial resolution is 131 pc. The set of basic equations are numerically solved by a parallel version of the Astrophysical Fluid Dynamics (AFD2) code (Mori et al. 2002). Here, we employ the AUSM-DV scheme (Wada and Liou 1997), which is a TVD scheme that can resolve the shock accurately. We use a tracer field advected with the same algorithm as the density in order to follow the metallicity of the gas. Also, the gas is assumed to be optically thin and in collisional ionization equilibrium. Radiative cooling losses are calculated self-consistently using the metallicity-dependent curves given by Sutherland and Dopita (1993).

Stars are assumed to form in rapidly cooling and Jeans unstable regions at a rate which is inversely proportional to the local free-fall time (Mori et al. 1999). When a star particle is formed, we identify this with approximately 10^4 single stars and distribute the associated mass of the star particle over the single stars according to Salpeter's initial mass function (Salpeter 1955). The lower and upper mass limits are taken as $0.1 M_\odot$ and $50 M_\odot$, respectively. When a star particle is formed and identified with a stellar assemblage as described above, stars more massive than $8 M_\odot$ start to explode as Type II supernovae (SNe) with the explosion energy of 10^{51} ergs and their outer layers are blown out with synthesized metals leaving the remnant of $1.4 M_\odot$. A mass of $2.4 M_\odot$ of oxygen and of $9.1 \times 10^{-2} M_\odot$ of iron are ejected from a Type II SN explosion (Tsujimoto et al. 1995). The ejected energy and well-mixed metals by SN are supplied to 8 local cells surrounding SN region.

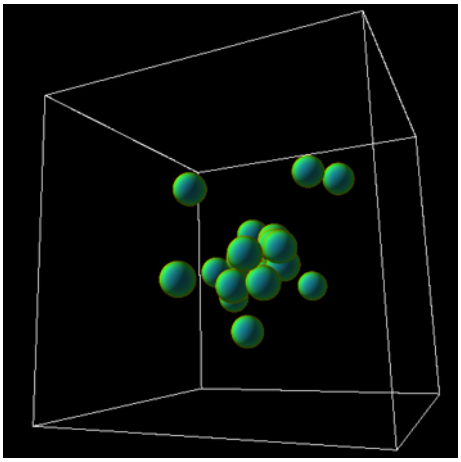

Fig. 1 Initial distribution of subgalactic condensations with a mass of $5.0 \times 10^9 M_\odot$ in a virial radius 8.6 kpc. The simulation *box* has a size of 134 kpc and the spatial resolution is 131 pc

3 Results

Figure 2 shows the snapshots of the gas density, the gas temperature distributions, and the gas metallicity [O/H] in a slice along the X–Y plane. The four panels in each low depict the time evolution from about 100 Myr to up to 1 Gyr. The density range is $-6 < \log(n/\mathrm{cm^{-3}}) < 1$, the temperature range is $3 < \log(T/\mathrm{K}) < 7.5$, and the metallicity range is $-5 < [\mathrm{O/H}] < 1$.

In the first 100 Myr, stars are formed in high-density peaks within subgalactic condensations and the burst of star formation starts. Then, massive stars in the star forming regions explode as SNe one after another, producing expanding hot bubbles surrounded by cooled dense shells. The gas in the vicinity of SNe is quickly enriched with ejected heavy elements, but a large amount of gas still retains low heavy-element abundance. Consequently, the metallicity distribution becomes highly inhomogeneous, where gas enriched as $[\mathrm{O/H}] \sim -1$ coexists with virtually primordial gas. The gas

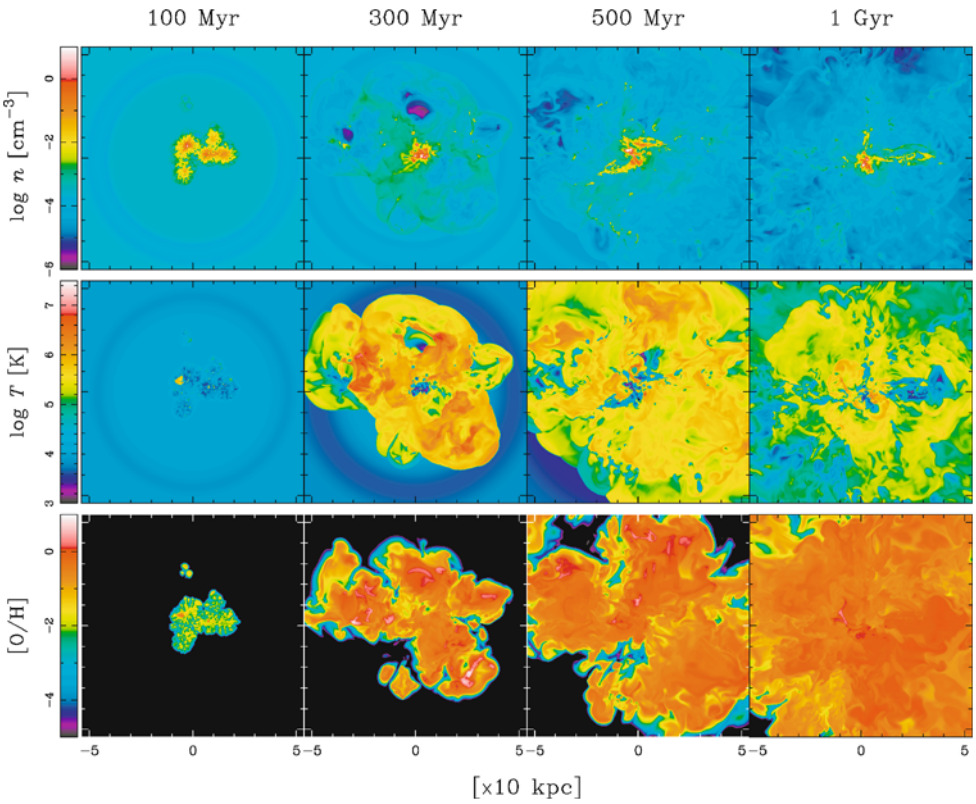

Fig. 2 Sectional distributions of the logarithmic number density of gas, the logarithmic temperature, and the oxygen abundance [O/H] of gas, respectively. The *four panels* in each low depict the time evolution of the simulation results until 1 Gyr

temperature increases up to about 10^8 K locally, and expanding hot bubbles of ∼kpc are produced; they are enclosed by cooled, dense shells. Subsequent SN explosions further accelerate the expansion of hot bubbles and the ambient gas is continuously swept up by the shells; the gas density increases further owing to the enhanced cooling rate in the dense shells. Since in the outer regions the density of the ISM is low, the bubble expansion is faster and SN-driven shock waves quickly collide with each other to generate super-bubbles of ∼50 kpc and the surrounding high-density, and the surrounding high-density, cooled ($T = 10^4$ K) shells form at 300 Myr. The hot bubbles expand further by subsequent SN explosions, and the shells sweep up the partially enriched ambient gas. The gas density in dense shells increases owing to the efficient radiative cooling mainly through the recombination and the collisional excitation of neutral hydrogen. The different initial topology of the multiphase ISM leaves an imprint also in the later evolutionary stages.

After 500 Myr, the hot bubbles blow out into the intergalactic space. This SN-driven galactic wind is an efficient mechanism to enrich the intergalactic medium with heavy elements over a large cosmological volume (see Mori et al. 2002). On the other hand, the dense shells undergoes hydrodynamic instabilities induced by shell–shell interactions and radiative cooling, eventually fragmenting into cold filaments and blobs. These interactions are giving rise to an intricate multiphase structure in the inner halo, where 10^{6-7} K gas coexists with a cooler 10^4 K phase from which it is separated by cooling interfaces. New stars are born in this enriched gas and again heavy elements are ejected from subsequent SNe. The rightmost panels show the structure at 1 Gyr. By this stage, the ISM is recycled repeatedly and about 72% of the initial gas has been processed into stars. Eventually, some amounts of cool, dense filaments are left at the center. But, the most of volume is filled with rarefied gas ($n \sim 10^{-4}$ cm^{-3}) that has intermediate temperature ($10^{4.5}$ K $< T < 10^{6.5}$ K). At this epoch, the mixing of heavy elements is nearly completed, and the metallicity of the remaining gas is a sub-solar value ($-1 <$ [O/H] < 0).

4 Discussion

We calculated the emission properties of the gas component assuming an optically thin gas in collisional ionization equilibrium using MAPPINGIII code written by Sutherland and Dopita (1993). Using the hydrogen number density, the gas temperature, and the gas metallicity at each grid point, we calculate the spectral energy distribution (SED) of the gas for the wavelength range of 1–10,000,000 Å. In practice, to obtain the SED of the system we sum up the SED of each grid point for the gas components. At the earliest stages of less than 300 Myr, the Lyα emission is conspicuous (it

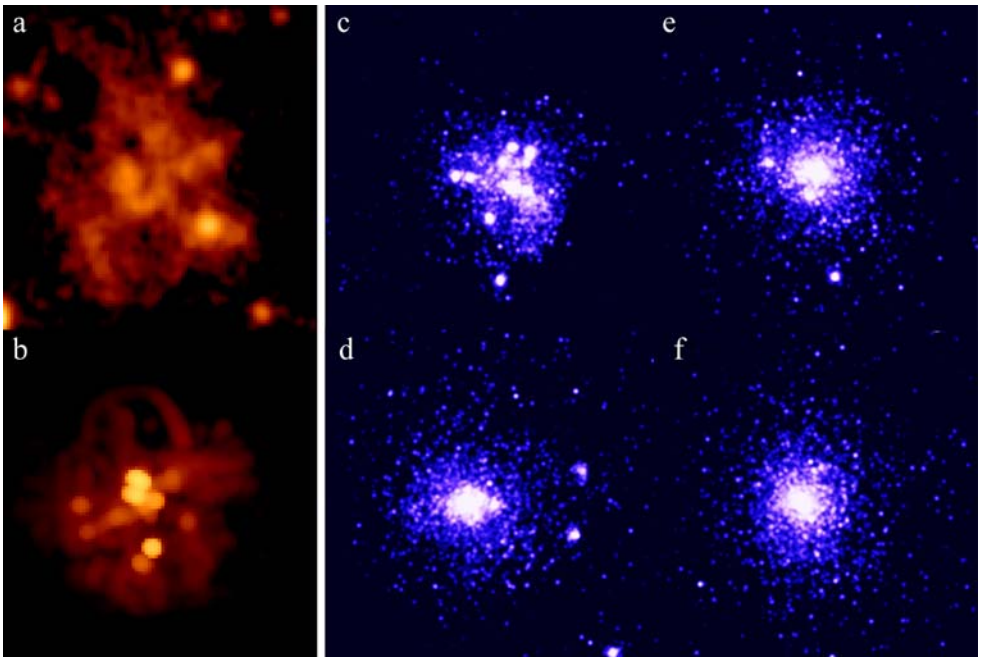

Fig. 3 *Left panels*: **a** Narrow-band image of extended LAE "LAB1" taken with the Subaru Telescope in the SSA22 field at the redshift $z = 3.09$ (Matsuda et al. 2004). **b** The projected distribution of Lyα emission from the gas component for the simulated galaxy at 200 Myr. The image is smoothed with a Gaussian kernel with a full-width at half-maximum of 7.6 kpc, which corresponds to 1.0″ at redshift $z = 3.09$, the same resolution (100 pixels × 100 pixels) as the observation. *Middle and right panels*: The projected distribution of stars at **c** 2.0 Gyr, **d** 2.4 Gyr, **e** 2.8 Gyr, and **f** 3.2 Gyr, respectively

comes from high-density cooling shells) and its luminosity is more than 10^{43} erg s^{-1}. The Lyα luminosity perfectly matches that observed in LAEs. This result suggests that LAEs could correspond to an early supernova-dominated phase before 300 Myr. Among theoretical models for LAEs, the present multiple supernova model is distinctive in having bubbly structure.

In Figs. 3a and 3b, the narrow-band image of extended LAE observed by Matsuda et al. (2004) is compared to the distribution of the Lyα emission of the simulated galaxy at 200 Myr. We find that the physical extent of ∼100 kpc and the bubbly structure produced by multiple supernovae are quite similar to the observed features in the Lyα surface brightness distribution of this LAE. After 300 Myr, the Lyα luminosity quickly declines to several times 10^{41} erg s^{-1}, as the emission from cooling gas decreases immediately owing to the leak of explosion energy through the blowouts of super-bubbles. We should note that Mori et al. (2004) demonstrated that Lyα extinction due to dust is negligible within the first 50 Myr because the metallicity of gas is very low. It is also the case for our simulation. But it is unclear for the later epoch. To know the escape fraction of Lyα photons, we need to calculate the three dimensional radiative transfer of Lyα emission with dust extinction. We realize that it is so challenging and important, but it is beyond the scope of this article. The full analysis including the contribution of dust extinction and emission will be given elsewhere.

Our simulation showed that the peak star formation rate is about $40 M_\odot$ yr^{-1} and the burst of star formation continues to 300 Myr (see Mori and Umemura 2006). These results are consistent with the stellar age determinations of LBGs derived by recent observations. The simulation successfully reproduced the metallicity of LBGs which is mostly subsolar and ranges from [Fe/H] ~ -0.3 to -1. The galaxy after 300 Myr is featured with diffuse, asymmetric structures, and outflows of $100 \sim 500$ km s^{-1}. These features look quite similar to those observed for LBGs (Pettini et al. 2001; Adelberger et al. 2003), where the low-ionization interstellar absorption lines of LBGs are blue shifted by hundreds km s^{-1} relative to systemic velocities and Lyα lines are redshifted to the same degree. In the light of such properties, the simulated post-starburst galaxy that has the age of 1 Gyr can correspond to LBGs.

The following dynamical evolution is studied by an N-body simulation with one million particles, to explore the end-product of this galaxy. Figures 3c–f show the snapshots of the projected distribution of star particles at the elapsed times of 2.0, 2.4, 2.8, and 3.2 Gyr, respectively. It is found that the assembly of sub-condensations and the virialization of the total system are almost completed in 3 Gyr, so that the system becomes in a quasi-equilibrium state. They have a large central concentration that well accords with de Vaucouleurs' $r^{1/4}$ profile (de Vaucouleurs 1948). The resultant absolute magnitude in blue band and visual band are $M_B = -17.2$ mag and $M_V = -18.0$ mag, respectively. The colour U–$V = 1.15$ and V–$K = 2.85$ are consistent with the colour-magnitude relation of elliptical galaxies in Coma cluster of galaxies (Bower et al. 1992). Furthermore, the combination of the surface brightness, the effective radius $r_e = 3.97$ kpc, and the central velocity dispersion $\sigma_0 = 133$ km s^{-1} is on the fundamental plane of elliptical galaxies within their scatters (Djorgovski and Davis 1987; Burstein et al. 1997).

By these comparisons of the simulation results with the observations, it is concluded that LAEs and LBGs correspond to infants of elliptical galaxies, and the on-going, major chemical enrichment phases of elliptical galaxies. In addition, we have shown that the metallicity reaches the level of solar abundance in the first 1 Gyr.

Acknowledgements This work was supported in part by the Grant-in-Aid of the JSPS, 14740132, and by Grants-in-Aid of the MEXT, 16002003. The computations reported here were performed on the Earth Simulator at the JAMSTEC, the SPACE at Senshu University, and the computational facilities at CCS in the University of Tsukuba.

References

Adelberger, K.L., et al.: Galaxies and intergalactic matter at redshift $z = 3$: Overview. Astrophys. J. **584**, 45 (2003)

Barnes, J., Efstathiou, G.: Angular momentum from tidal torques. Astrophys. J. **319**, 575 (1987)

Blumenthal, G.R., Faber, S.M., Primack, J.R., Rees, M.J.: Formation of galaxies and large-scale structure with cold dark matter. Nature **311**, 517 (1984)

Bower, R.G., Lucey, J.R., Ellis, R.S.: Precision photometry of early type galaxies in the Coma and Virgo clusters—a test of the universality of the colour/magnitude relation—Part two—analysis. Mon. Not. Roy. Astron. Soc. **254**, 601 (1992)

Burstein, D., Bender, R., Faber, S., Nolthenius, R.: Global relationships among the physical properties of stellar systems. Astron. J. **114**, 1365 (1997)

de Vaucouleurs, G.: Recherche sur les nebuleuses extragalactiques. Ann. Astrophys. **11**, 247 (1948)

Dey, A., et al.: A galaxy at $z = 5.34$. Astrophys. J. **498**, L93 (1998)

Djorgovski, S., Davis, M.: Fundamental properties of elliptical galaxies. Astrophys. J. **313**, 59 (1987)

Giavalisco, M.: Lyman-break galaxies. Annu. Rev. Astron. Astrophys. **40**, 579 (2002)

Matsuda, Y., et al.: A SUBARU search for Ly£ blobs in and around the protocluster region at redshift $z = 3.1$. Astron. J. **128**, 569 (2004)

Mori, M., Umemura, M.: The evolution of galaxies from primeval irregulars to present-day ellipticals. Nature **440**, 644 (2006)

Mori, M., Yoshii, Y., Tsujimoto, T., Nomoto, K.: The evolution of dwarf galaxies with star formation in an outward-propagating super-shell. Astrophys. J. **478**, L21 (1997)

Mori, M., Yoshii, Y., Nomoto, K.: Dissipative process as a mechanism of differentiating internal structures between dwarf and normal elliptical galaxies in a cold dark matter universe. Astrophys. J. **511**, 585 (1999)

Mori, M., Ferrara, A., Madau, P.: Early metal enrichment by pregalactic outflows. II. Three-dimensional simulations of blow-away. Astrophys. J. **571**, 40 (2002)

Mori, M., Umemura, M., Ferrara, A.: The nature of Ly£ blobs: supernova-dominated primordial galaxies. Astrophys. J. **613**, L97 (2004)

Navarro, J.F., Frenk, C.S., White, S.D.M.: A universal density profile from hierarchical clustering. Astrophys. J. **490**, 493 (1997)

Pettini, M., et al.: The rest-frame optical spectra of Lyman break galaxies: star formation, extinction, abundances, and kinematics. Astrophys. J. **554**, 981 (2001)

Salpeter, E.E.: The luminosity function and stellar evolution. Astrophys. J. **121**, 161 (1955)

Steidel, C.C., et al.: Spectroscopic confirmation of a population of normal star-forming galaxies at redshifts $z > 3$. Astron. J. **112**, 352 (1996)

Sutherland, R.S., Dopita, M.A.: Cooling functions for low-density astrophysical plasmas. Astrophys. J. Suppl. Ser. **88**, 253 (1993)

Tanighichi, Y., et al.: Lyman emitters beyond redshift 5: The dawn of galaxy formation. J. Korean Astron. Soc. **36**, 123 (2003)

Tsujimoto, T., et al.: Relative frequencies of type Ia and type II supernovae in the chemical evolution of the Galaxy, LMC and SMC. Mon. Not. Roy. Astron. Soc. **277**, 945 (1995)

Wada, Y., Liou, M.-S.: An accurate and robust flux splitting scheme for shock and contact discontinuities. SIAM J. Sci. Comput. **18**, 633 (1997)